International Journal of Simulation, Optimization & Modelling
ISSN: 3083-967X

Investigation of Fuel Nozzle Performance on Direct Injection Diesel Engines Using Computational Simulation

Rosli Abu Bakar[1], Semin[1], Muhibbuddin[2], Mahyuddin[3]

[1]Faculty of Mechanical and Automotive Engineering Technology, Universiti Malaysia Pahang Al Sultan Abdullah, 26600, Malaysia
[2]Department of Mechanical and Industrial Engineering, Universitas Syiah Kuala, Banda Aceh, 23111, Indonesia
[3]Department of Mechanical Engineering, Universitas Abulyatama Aceh, Aceh Besar, 23372, Indonesia

Corresponding Author: muhib@usk.ac.id

Abstract
Single-cylinder model simulation designed for four-stroke direct-injection diesel engines requires advanced analysis of the performance effect of the direct-injection diesel engine model, focusing on fuel nozzle multi-hole geometries. The computational model simulation development used the commercial computational fluid dynamics of GT-POWER 6.2 software, specially developed for internal combustion engine performance simulation. The research concentrated on the one-dimensional model and focused on the variation of fuel nozzle multi-hole geometries developed from all of the engine components' size measurements of the original selected diesel engine. All the measurement data is inputted to the window engines component menu to run input data in the model. Results of the diesel engine fuel nozzle multi holes geometries model simulation running are in GT-POST. The model performance is shown in the engine cylinder and engine crank-train on the software window output. The performance analysis effect of the model investigated the fuel in-cylinder engine, indicating the model's specific fuel consumption, torque, and power. The simulation showed that the seven-hole nozzle provided the best burning for fuel in-cylinder burn, and the five-hole nozzle provided the best for indicated power, indicated torque, and indicated specific fuel consumption at any different engine speed in the simulation.

Article Info
Received: 05 April 2025
Revised: 02 May 2025
Accepted: 04 May 2025
Available online: 21 May 2025

Keywords
Diesel engine
Fuel nozzle holes
Computational
Simulation
Performance

1. Introduction

The four-stroke direct-injection diesel engine was measured and modelled using the GT-POWER computational model and explored single-cylinder diesel engine performance effect based on engine rpm (Muhibbuddin, Muchlis, Syarif, & Jalaludin, 2025; Nizar, Yana, Bahagia, & Yusop, 2025; Semin, Ismail, & Ali, 2007). GT-POWER is the leading engine simulation tool used by engine and vehicle makers and suppliers and is suitable for the analysis of a wide range of engine issues (Muchlis, Efriyo,

Rosdi, & Syarif, 2025; Rosdi, Ghazali, & Yusop, 2025; Smulter, 2024). The details of the diesel engine design vary significantly over the engine performance and size range. Different combustion chamber geometries and fuel injection characteristics are required to deal effectively with major diesel engine design problems, achieving sufficiently rapid fuel-air mixing rates to complete the fuel-burning process in the time available. A wide variety of inlet port geometries, cylinder head and piston shapes, and fuel-injection patterns are used to accomplish this over the diesel size range (Muchlis, Efriyo, Rosdi, Syarif, & Leman, 2025; Sardjono, Khoerunnisa, Rosdi, & Muchlis, 2025; Van Basshuysen & Schäfer, 2016). The engine ratings usually indicate the highest power at which manufacturers expect their products to give satisfactory power, economy, reliability and durability under service conditions. Heywood usually also gives maximum torque and the speed at which it is achieved. Diesel engine performance parameters are essential due to geometrical properties, efficiency, and other related parameters. The engine efficiencies are indicated as thermal efficiency, brake thermal efficiency, mechanical efficiency, volumetric efficiency and relative efficiency (Kirkpatrick, 2020; Maulana, Rosdi, & Sudrajad, 2025; Rosdi, Yasin, Khayum, & Maulana, 2025). The other related engine performance parameters are mean adequate pressure, mean piston speed, specific power output, specific fuel consumption, intake valve mach index, fuel-air or air-fuel ratio and calorific value of the fuel (Bakar & Semin, n.d.; Khalisha, Caisarina, & Fakhrana, 2025; Muhtadin, Rosdi, Faisal, Erdiwansyah, & Mahyudin, 2025). The diesel engine compression ratio is defined as the maximum cylinder volume (the displaced or swept volume plus the clearance volume) divided by the minimum cylinder volume (Heywood, 1988; Jalaludin, Kamarulzaman, Sudrajad, Rosdi, & Erdiwansyah, 2025; Rosdi, Maghfirah, Erdiwansyah, Syafrizal, & Muhibbuddin, 2025). The power the diesel engine delivers, and the dynamometer absorbs is the product of torque and angular speed. The engine efficiencies are defined by (Grimaldi & Millo, 2015). This research investigates the performance effect of fuel nozzle hole material geometries on the engine, indicating power, torque, fuel consumption, and fuel in the engine cylinder.

The diesel engine compression ratio is defined as the maximum cylinder volume, which is the sum of the displaced volume (Vd) and the clearance volume (Vc) divided by the minimum cylinder volume (Vc) (Grimaldi & Millo, 2015). The diesel engine compression ratio:

$$r_c = \frac{V_d + V_c}{V_c} \tag{1}$$

The power the diesel engine delivers, and the dynamometer absorbs is the product of torque and angular speed. Diesel engine power definition as :

$$P = 2\pi NT \tag{2}$$

In engine efficiencies, every efficiency is defined by (Rajput, 2005). Indicated thermal efficiency (η_{ith}) is the ratio of energy (E) in the stated power (ip) to the input fuel energy. Brake thermal efficiency (η_{bth}) is the energy ratio in the brake power (bp). Mechanical efficiency (η_m) is defined as the ratio of brake power (bp) or delivered power to the indicated power (ip) or power provided to the piston, and it can also be defined as the ratio of the brake thermal efficiency to the indicated thermal efficiency. Relative efficiency or efficiency ratio (η_{rel}) is the thermal efficiency ratio of an actual cycle to that of the ideal cycle. The efficiency ratio is an advantageous criterion indicating the engine's degree of development. One of the fundamental parameters that determine the performance of four-stroke engines is the volumetric efficiency (ηv), as four-stroke engines have a distinct suction stroke, and the volumetric efficiency indicates the breathing ability of the engine (Khayum, Goyal, & Kamal, 2025; Kumari & Badholiya, 2020; Muhibbuddin, Hamidi, & Fitriyana, 2025). Volumetric efficiency is defined as the volume flow rate of air into the intake system divided by the rate at which the system displaces the volume. The normal range of volumetric efficiency at full throttle for SI engines is 80% to 85%, and for CI engines is 85% to 90%.

$$\eta_{ith} = \frac{ip}{E} \tag{3}$$

$$\eta_{bth} = \frac{bp}{E} \tag{4}$$

$$\eta_{m} = \frac{bp}{ip} \tag{5}$$

$$\eta_{v} = \frac{\dot{m}_a}{\rho_a V_{disp} N/2} \tag{6}$$

$$\eta_{rel} = \frac{\text{Actual thermal efficiency}}{\text{Air - standard efficiency}} \tag{7}$$

The other related engine performance was defined (Iqbal, Rosdi, Muhtadin, Erdiwansyah, & Faisal, 2025; Selvakumar, Maawa, & Rusiyanto, 2025; Zhou, Sofianopoulos, Lawler, & Mamalis, 2020). Mean adequate pressure (*mep*) where n_R is the number of crank revolutions for each power stroke per cylinder (two for four-stroke, one for two-stroke cycles) as :

$$mep = \frac{Pn_R}{V_d N} \tag{8}$$

The measure of an engine's efficiency, which will be called the fuel conversion efficiency, is given by (Heywood, 1988):

$$nf = \frac{W_c}{m_f Q_{HV}} = \frac{(Pn_R / N)}{(m_f n_R / N) Q_{HV}} = \frac{P}{m_f Q_{HV}} \tag{9}$$

Specific fuel consumption as:

$$sfc = \frac{m_f}{P} \tag{10}$$

In engine testing, the air mass flow rate m_a and the fuel mass flow rate m_f are typically measured. The ratio of these flow rates helps define engine operating conditions: air/fuel ratio (A/F) and fuel/air ratio (F/A). The following relationships between diesel engine performance parameters can be developed. For power *P*:

$$P = \frac{\eta_f m_a N Q_{HV} (F/A)}{n_R} \tag{11}$$

$$P = \frac{\eta_f \eta_v N V_d Q_{HV} \rho_{a,i} (F/A)}{2} \tag{12}$$

For torque T:

$$T = \frac{\eta_f \eta_v V_d Q_{HV} \rho_{a,i} (F/A)}{4\pi} \tag{13}$$

For mean adequate pressure:

$$mep = \eta_f \eta_v Q_{HV} \rho_{a,i} (F/A) \tag{14}$$

The specific power or the power per unit piston area is a measure of the engine designer's success in using the available piston area regardless of cylinder size. The specific power is:

$$\frac{P}{A_p} = \frac{\eta_f \eta_v N L Q_{HV} \rho_{a,i} (F/A)}{2} \tag{15}$$

Mean piston speed :

$$\frac{P}{A_p} = \frac{\eta_f \eta_v N \overline{S_p} Q_{HV} \rho_{a,i} (F/A)}{4} \tag{16}$$

The specific power is proportional to the product of the adequate pressure and the mean piston speed (Mufti, Irhamni, & Darnas, 2025; Mutlu & Kiliç, 2016; Rosli, Xiaoxia, & Shuai, 2025). These relationships illustrate the direct importance to engine performance of high fuel conversion efficiency, high volumetric efficiency, increasing the output of a given displacement engine by increasing the inlet air density, maximum fuel/air ratio that can be useful burned in the engine and high mean piston speed.

2. Methodology

The development of the single cylinder modeling and simulation for a four-stroke direct-injection (DI) diesel engine was presented in this paper. The specification of the selected diesel engine model is presented in **Table 1**. The development of the GT-POWER of single-cylinder four-stroke direct-injection diesel engine modelling is done step by step. The first step is to open all of the selected diesel engine components to measure the engine component's part size. Then, the engine components size data will be inputted into the GT-POWER library of all-engine components data.

To create the GT-POWER model, select window and then Tile with Template Library from the menu. This will place the GT-POWER template library on the left-hand side of the screen. The template library contains all available templates that can be used in GT-POWER. Some of these templates needed in the project must be copied into the project before they can be used to create objects and parts. To this model, click on the icons listed and drag them from the template library into the project library. Some of these are templates, and some are objects that have already been defined and included in the GT-POWER template library (Febrina & Anwar, 2025; Pranoto, Rusiyanto, & Fitriyana, 2025; Salih & DelVescovo, 2018). This research focuses on the fuel nozzle hole of the fuel injector and the engine modelling according to Bakar, shown in **Fig. 1** (Bakar & Semin, n.d.). All of the parameters in the model will be listed automatically in the case setup, and each must be defined for the first case of the simulation. The physical of the fuel nozzle hole material detailed in the research is shown in **Fig. 2**. This figure shows the details of the injection hole or fuel nozzle hole. The fuel nozzle holes would be changed in wide of diameter hole and in different number.

Table 1. Specification of the selected diesel engine

Engine Parameters	Value	Engine Parameters	Value
Model	CF186F	Intake valve close (^{0}CA)	530
Bore (mm)	86.0	Exhaust valve open (^{0}CA)	147
Stroke (mm)	70.0	Exhaust valve close (^{0}CA)	282
Displacement (cc)	407.0	Maximum intake valve open (mm)	7.095
Number of cylinders	1	Maximum exhaust valve open (mm)	7.095
Connecting rod length (mm)	118.1	Valve lift periodicity (deg)	360
Piston pin offset (mm)	1.00	Fuel nozzle diameter (mm)	0.1
Intake valve open (^{0}CA)	395	Fuel nozzle hole number (pc)	4

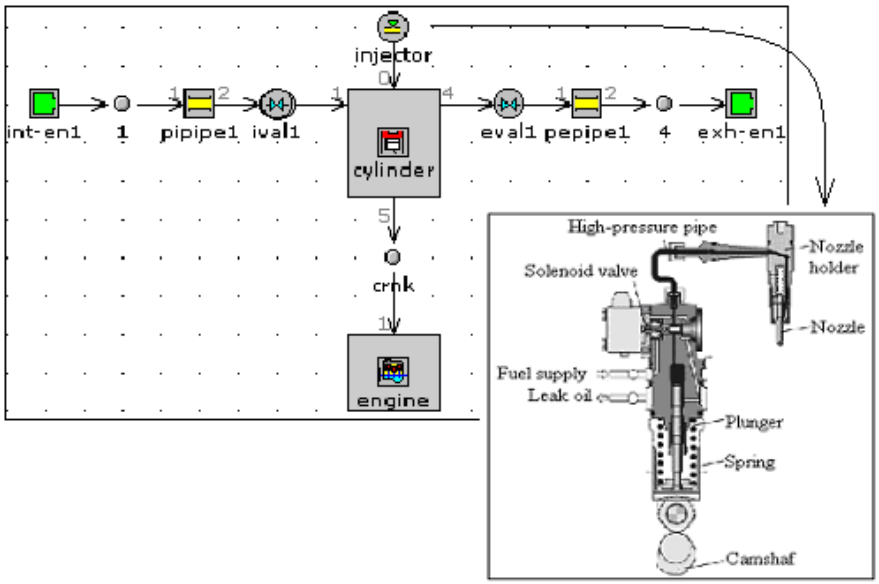

Fig. 1. Direct-injection single-cylinder diesel engine modelling using GT-Power

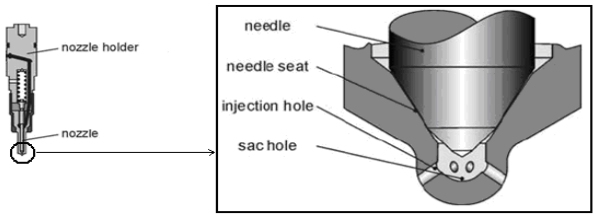

Fig. 2. Fuel nozzle holes detail

3. Result & Discussion

Produces several output files that contain simulation results in various formats. Most of the output is available in the post-processing application GT-POST. GT-POST is a powerful tool that can be used to view animation and order analysis output (Almardhiyah, Mahidin, Fauzi, Abnisa, & Khairil, 2025; Khanyi, Inambao, & Stopforth, 2025; Sumarno, Fikri, & Irawan, 2025). After the simulation, report tables that summarize the simulations can be produced. These reports contain important information about the simulation and simulation results in a tabular form. The computational simulation of the engine model results informs the engine performance. The running simulation result of this research focuses on the engine performance data based on variations of fuel nozzle material hole diameter size, diameter number, and engine speed (rpm). The diesel engine model was running at different engine speeds in rpm, which are 500, 1000, 1500, 2000, 2500, 3000, and 3500. The variations in fuel nozzle material hole numbers are multi-holes and several-number holes. The simulation model starts from the fuel nozzle with 1 – 10 holes, where the fuel nozzle has four holes.

Nozzle Holes Effect in Engine Cylinder Fuel

The simulation results from every case show that case 1 is at 500 rpm until case 8 at 4000 rpm. Numerous studies have suggested that decreasing the injector nozzle orifice diameter is an effective method of increasing fuel-air mixing during injection (Baik, Blanchard, & Corradini, 2003; Muzakki & Putro, 2025; NOOR, Arif, & Rusirawan, 2025). Smaller nozzle holes were found to be the most efficient at fuel/air mixing primarily because the fuel-rich core of the jet is smaller. In addition, decreasing the nozzle hole orifice diameter would reduce the length of the potential core region. Unfortunately,

decreasing nozzle hole size causes a reduction in the turbulent energy generated by the jet. Since fuel-air mixing is controlled by turbulence generated at the jet boundary layer, this will offset the benefits of the reduced jet core size.

Furthermore, jets emerging from smaller nozzle orifices were shown not to penetrate as far as those emerging from larger orifices. This decrease in penetration means that the fuel will not be exposed to all the available air in the chamber. For minimal nozzle size, the improvements in mixing related to decreased plume size may be negated by a reduction in radial penetration (Bahagia, Nizar, Yasin, Rosdi, & Faisal, 2025; Baumgarten, 2006; Nizar, Syafrizal, et al., 2025). This behaviour is undesirable because it restricts penetration to the chamber extremities where a large portion of the air mass resides. Furthermore, it hampers air entrainment from the head side of the plume because the exposed surface area is reduced. It has been suggested that a nozzle containing many small holes would provide better mixing than a nozzle consisting of a single large hole. The performance effect of fuel nozzle hole number and geometries of in-cylinder engine liquid fuel are shown in **Fig. 3 - 12**.

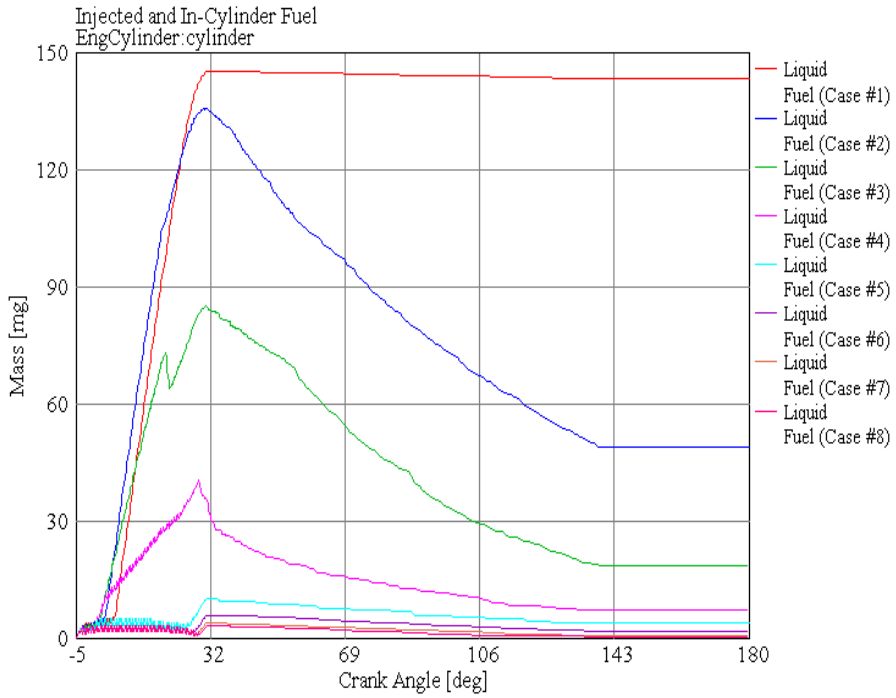

Fig. 3. In-cylinder liquid fuel of nozzle one hole

Fig. 3 illustrates the distribution of in-cylinder liquid fuel mass for a single-hole nozzle configuration against crank angle (Crank Angle). In all cases, the liquid fuel mass sharply increases shortly after the start of injection at around -5 degrees crank angle. In Case #1 (blue line), the liquid fuel mass reaches the highest peak of approximately 135 mg at a crank angle of 32 degrees before gradually decreasing. Case #2 (green line) peaks at around 85 mg, while Case #3 (pink line) reaches a maximum of approximately 30 mg. Meanwhile, the other cases (#4 to #8) show much lower fuel accumulation, generally not exceeding 10 mg. The decrease in liquid fuel mass after 32 degrees indicates the processes of evaporation and combustion inside the cylinder. In Case #1, although a decline occurs, the liquid fuel mass remains above 60 mg until nearly 143 degrees.

In contrast, in Cases #2 and #3, the fuel mass decreases rapidly and almost entirely evaporate before 143 degrees. This behaviour suggests that different operating conditions (such as injection pressure, temperature, or nozzle design) significantly affect the evaporation characteristics of the fuel. Case #1 appears to retain liquid fuel for a longer duration, which could imply slower combustion or potential incomplete combustion if not properly optimized.

Fig. 4 presents the in-cylinder liquid fuel mass for a two-hole nozzle configuration as a function of crank angle. It is evident that Cases #1 and #2 exhibit a very rapid rise in liquid fuel mass starting around -5 degrees crank angle, reaching peaks of approximately 165 mg and 150 mg, respectively, by around 32 degrees. Unlike the one-hole nozzle results, the liquid fuel mass in Cases #1 and #2 remains almost constant with minimal evaporation until the end of the crank angle range (180 degrees). Case #3 (green line) peaks around 45 mg and gradually declines, indicating a more active evaporation process than Cases #1 and #2. For the other cases (#4 to #9), the maximum liquid fuel mass remains relatively low, generally below 10 mg, and declines steadily after the peak. The high liquid fuel mass retention in Cases #1 and #2 suggests that the two-hole nozzle configuration may produce larger fuel droplets or slower evaporation under certain conditions, potentially affecting combustion efficiency. In contrast, the faster decline in Case #3 and the lower fuel mass in the remaining cases suggest better atomization and evaporation characteristics under their respective conditions.

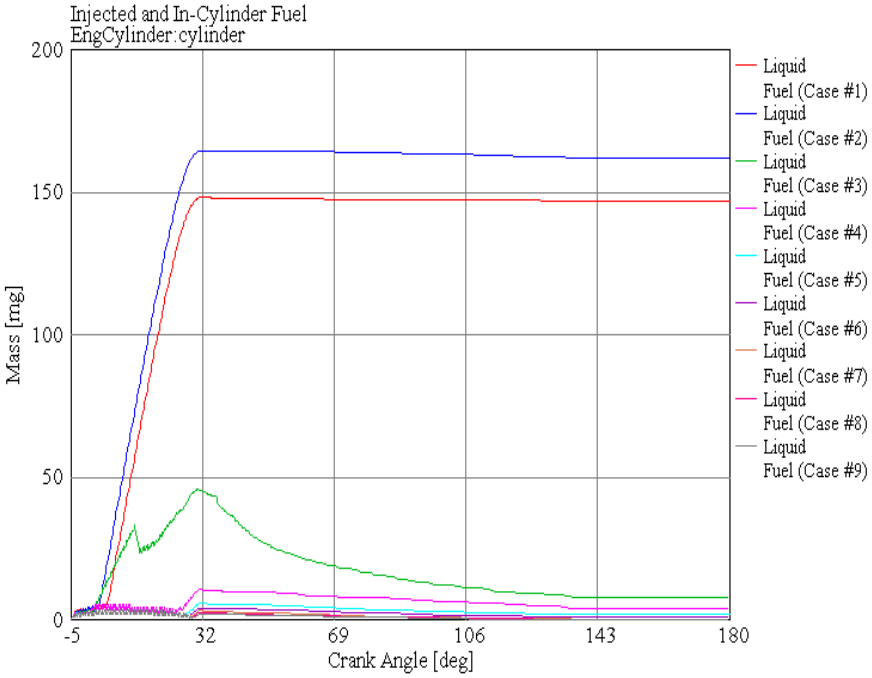

Fig. 4. In-cylinder liquid fuel of nozzle two holes

Fig.5 displays the in-cylinder liquid fuel mass for a three-hole nozzle configuration across the crank angle range. Like the two-hole configuration in Figure 4, Cases #1 and #2 show rapid increases in fuel mass, reaching peaks of approximately 165 mg and 150 mg around 32 degrees crank angle, respectively. These values remain nearly constant throughout the cycle, up to 180 degrees, indicating minimal evaporation. On the other hand, case #3 (green line) peaks around 30 mg and gradually decreases, reflecting a higher evaporation rate. This consistent behaviour from Case #3 across nozzle configurations may suggest sensitivity to operating conditions such as pressure or temperature.

In contrast, Cases #4 to #8 maintain low fuel masses (mostly below 10 mg) and exhibit gradual reductions after injection. These findings reinforce the trend that increasing nozzle holes does not necessarily guarantee improved evaporation. While more holes may enhance spray coverage, fuel atomization and vaporization depend heavily on injection parameters and combustion chamber conditions. The similar retention of high liquid fuel mass in Cases #1 and #2 between Figures 4 and 5 also suggests that nozzle configuration must be coupled with optimized injection strategies for efficient combustion.

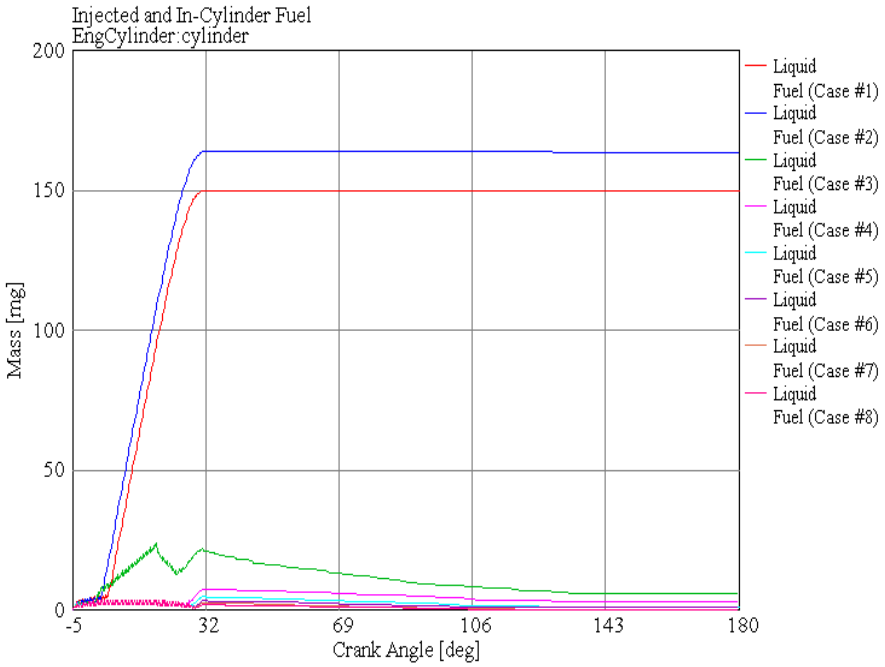

Fig. 5. In-cylinder liquid fuel of nozzle three holes

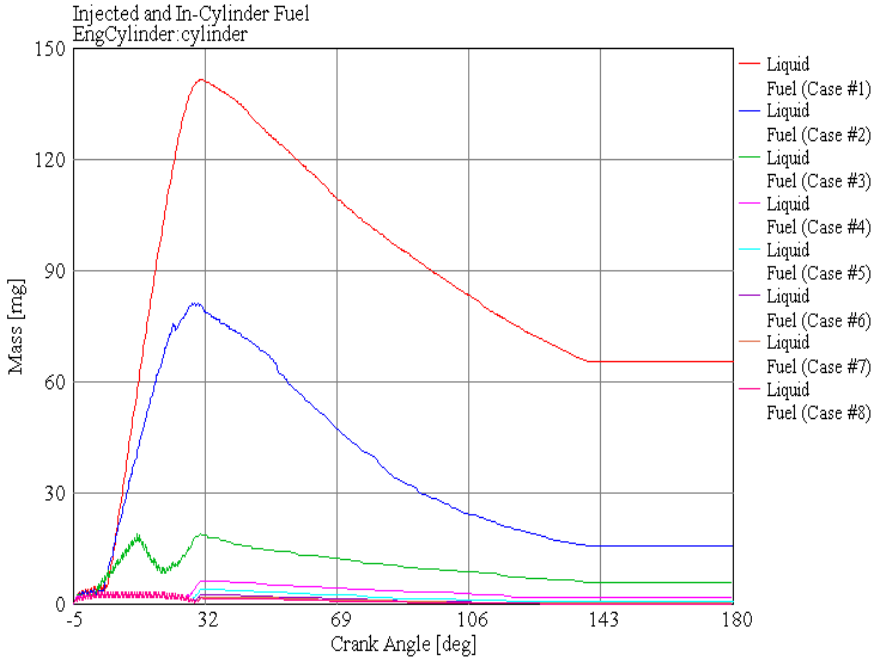

Fig. 6. In-cylinder liquid fuel of nozzle four holes

Fig. 6 illustrates a four-hole nozzle configuration's in-cylinder liquid fuel mass behaviour. In contrast to Figures 4 and 5, Case #1 (red line) in this graph shows a higher peak of approximately 140 mg at around 32 degrees crank angle, followed by a consistent and steady decrease down to about 65 mg at 143 degrees, indicating a significant degree of fuel evaporation. Case #2 (blue line) follows a similar trend, peaking at around 85 mg and decreasing to approximately 25 mg over time. Compared to the two-hole and three-hole configurations, these results show better evaporation performance, likely due to finer atomization and improved in-cylinder air-fuel mixing. Cases #3 to #8 all exhibit low peak fuel

mass levels, generally staying below 20 mg and steadily declining as the crank angle increases. The four-hole nozzle configuration seems to strike a balance between sufficient fuel injection and effective evaporation. Notably, the sharp reduction in liquid mass after peak injection in Case #1 suggests enhanced combustion readiness, which could lead to more efficient and complete combustion. This improvement implies that increasing the number of nozzle holes beyond three can contribute to more favourable in-cylinder fuel behaviour, provided the injection parameters are well-tuned.

Fig. 7 shows the in-cylinder liquid fuel mass for a five-hole nozzle configuration across the crank angle range. Case #1 (red line) reaches a peak of approximately 155 mg at around 32° crank angle and remains nearly constant throughout the cycle up to 180°, showing almost no evaporation. Case #2 (blue line), however, peaks at approximately 70 mg and demonstrates a consistent downward trend, decreasing to about 20 mg, which indicates active evaporation and better vapour-phase mixing. Case #3 (green line) reaches a maximum of around 15 mg, then gradually declines, while the remaining cases (#4 to #8) have very low peak values (typically under 10 mg) and steady decay patterns. Compared to the four-hole configuration, the five-hole nozzle results in higher peak fuel mass retention in Case #1, suggesting that increased nozzle count may contribute to larger droplet formation or less effective atomization under certain conditions. Although Case #2 shows good evaporation, the consistently high liquid mass in Case #1 may pose a risk of incomplete combustion if not properly optimized. These findings imply that while five-hole injectors can deliver a high fuel mass, achieving balanced atomization and evaporation may require more precise control over injection pressure and spray targeting.

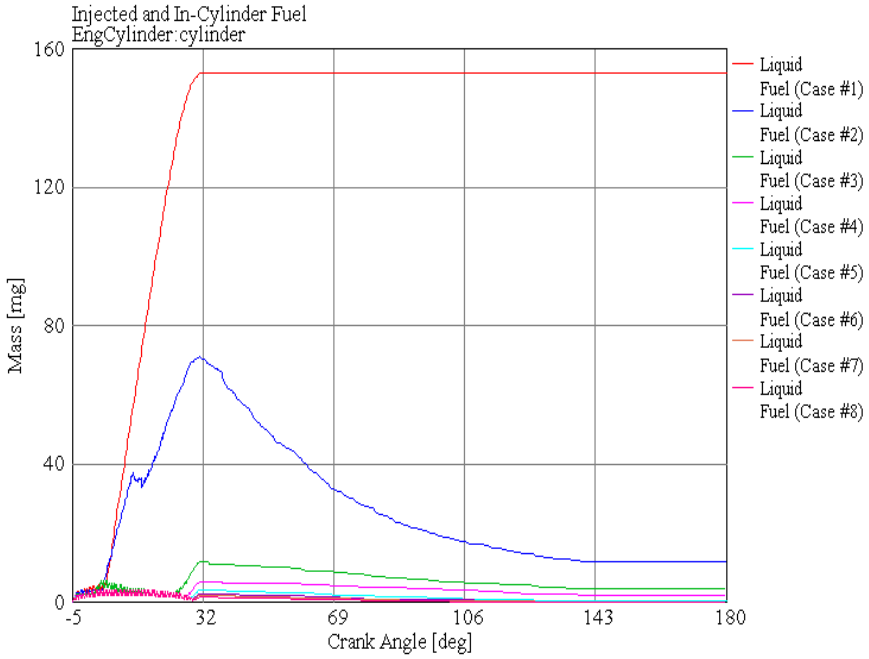

Fig. 7. In-cylinder liquid fuel of nozzle five holes

Fig. 8 presents the in-cylinder liquid fuel mass for a six-hole nozzle configuration as a function of crank angle. Case #1 (red line) peaks at approximately 155 mg near a 32° crank angle, gradually decreasing to around 125 mg by 143°, suggesting moderate evaporation. Case #2 (blue line) reaches about 110 mg and maintains a relatively stable value, with only a slight reduction, implying slower evaporation. Case #3 (green line) shows a small peak just below 15 mg, followed by a gradual decay, while the remaining cases (#4 to #8) stay under 10 mg and decline steadily throughout the crank cycle. Compared to the five-hole configuration, the six-hole nozzle maintains similar trends in terms of initial fuel mass and evaporation rate, especially for Cases #1 and #2. However, the evaporation performance appears less aggressive than in the four-hole setup (Figure 6), which showed a more significant drop in fuel mass

post-injection. This could be due to droplet overlap or insufficient in-cylinder mixing with increased nozzle holes. Thus, while the six-hole nozzle can deliver a high mass of fuel quickly, its effectiveness in vaporizing that fuel within the optimal combustion window might require further optimization of injection parameters such as timing, pressure, and angle.

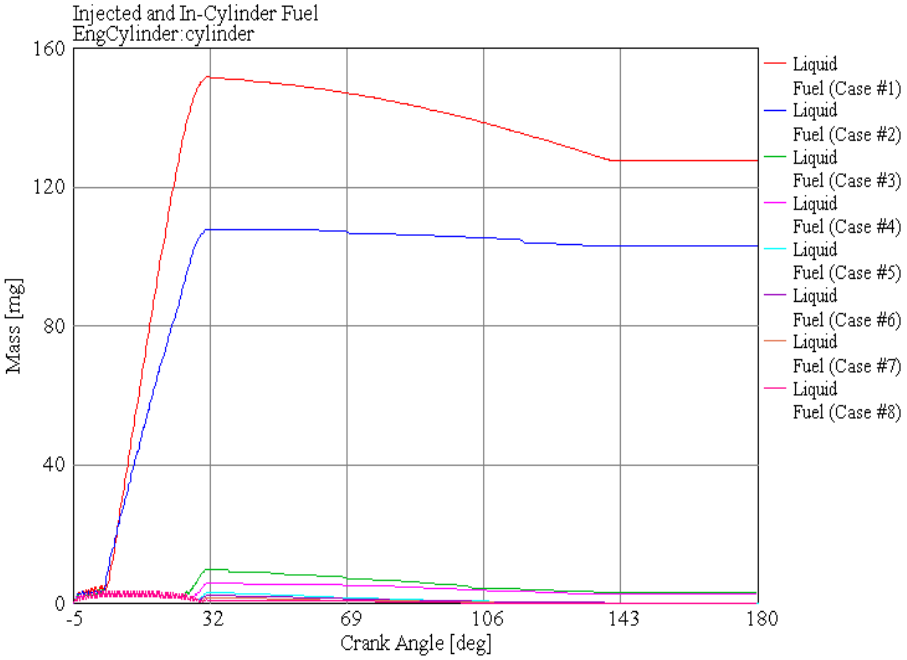

Fig. 8. In-cylinder liquid fuel of nozzle six holes

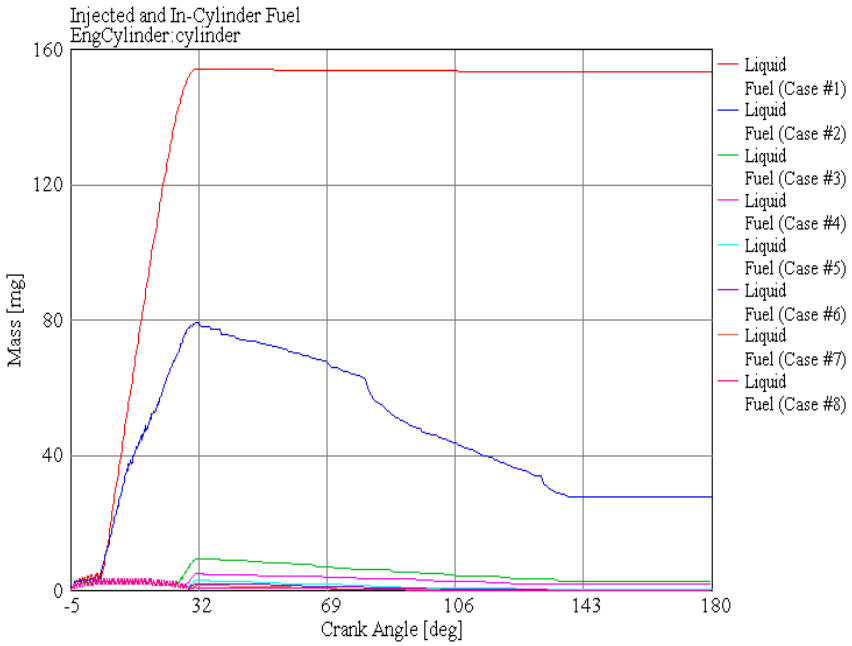

Fig. 9. In-cylinder liquid fuel of nozzle seven holes

Fig. 9 presents the in-cylinder liquid fuel mass distribution for a seven-hole nozzle configuration. Case #1 (red line) peaks at around 155 mg shortly after injection (approximately 32° crank angle) and remains nearly constant throughout the combustion cycle up to 180°, indicating minimal evaporation. In contrast, Case #2 (blue line) shows a peak of around 85 mg and gradually decreases to 30 mg, indicating

active evaporation. Case #3 (green line) maintains a relatively low peak under 15 mg and follows a steady decline, while the remaining cases (#4 to #8) stay under 10 mg with smooth decay patterns, similar to prior configurations. This figure indicates that increasing the number of nozzle holes beyond six does not significantly improve evaporation behaviour in the early combustion phase, especially for Case #1, which shows persistent fuel mass retention. The evaporation trend for Case #2 in this setup is consistent with earlier figures, reflecting effective atomization but possibly limited by in-cylinder air interaction or spray impingement. Overall, the seven-hole configuration provides no substantial advantage over the four- or six-hole designs and may introduce challenges related to over-fueling or poor air-fuel mixing if not carefully optimized.

Fig. 10 illustrates the in-cylinder liquid fuel mass for an eight-hole nozzle configuration across the crank angle. Case #1 (red line) exhibits the highest peak at approximately 155 mg by 32° crank angle and remains constant until 180°, indicating virtually no evaporation. In contrast, Case #2 (blue line) peaks at about 70 mg and steadily decreases to 20 mg, showing moderate evaporation throughout the cycle. Case #3 (green line) peaks at less than 10 mg and rapidly declines, while the remaining cases (#4 to #8) remain very low, generally under 5 mg, and follow similar decay patterns. Despite the increase in the number of nozzle holes, the results do not show significant improvement in fuel evaporation compared to the four- or five-hole configurations. The retained mass in Case #1, which does not evaporate significantly, may result in incomplete combustion. Meanwhile, Case #2 still demonstrates effective atomization and evaporation behaviour, consistent across all configurations. These findings suggest that increasing the number of nozzle holes enhances spray distribution. However, there is a trade-off with droplet size and in-cylinder mixing quality, potentially limiting evaporation efficiency beyond a certain point.

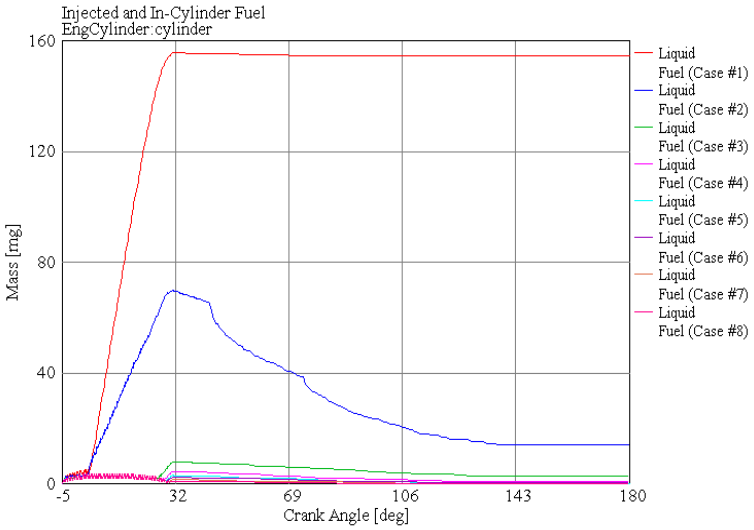

Fig.10. In-cylinder liquid fuel of nozzle eight holes

Fig.11 depicts a nine-hole nozzle configuration's in-cylinder liquid fuel mass distribution. Case #1 (red line) rapidly reaches a peak of approximately 155 mg near the 32° crank angle and remains flat at 180°, indicating no evaporation throughout the cycle. Case #2 (blue line) peaks at around 115 mg and similarly shows a constant trend, contrasting with earlier configurations where evaporation was more evident. Case #3 (green line) reaches about 10 mg and slowly decreases, while Cases #4 to #8 display very low mass values (typically below 5 mg) and follow a consistent downward trend. While offering the highest number of nozzle holes, this configuration demonstrates the least fuel evaporation in its top cases (especially Case #1 and Case #2), indicating potential issues with droplet impingement, oversaturation, or inadequate air-fuel mixing. The persistent high fuel mass could lead to poor combustion efficiency or increased unburned hydrocarbon emissions. Overall, Figure 11 suggests that

simply increasing the number of nozzle holes beyond a certain point—without optimizing other factors like injection pressure or spray targeting—can negatively impact in-cylinder evaporation behaviour.

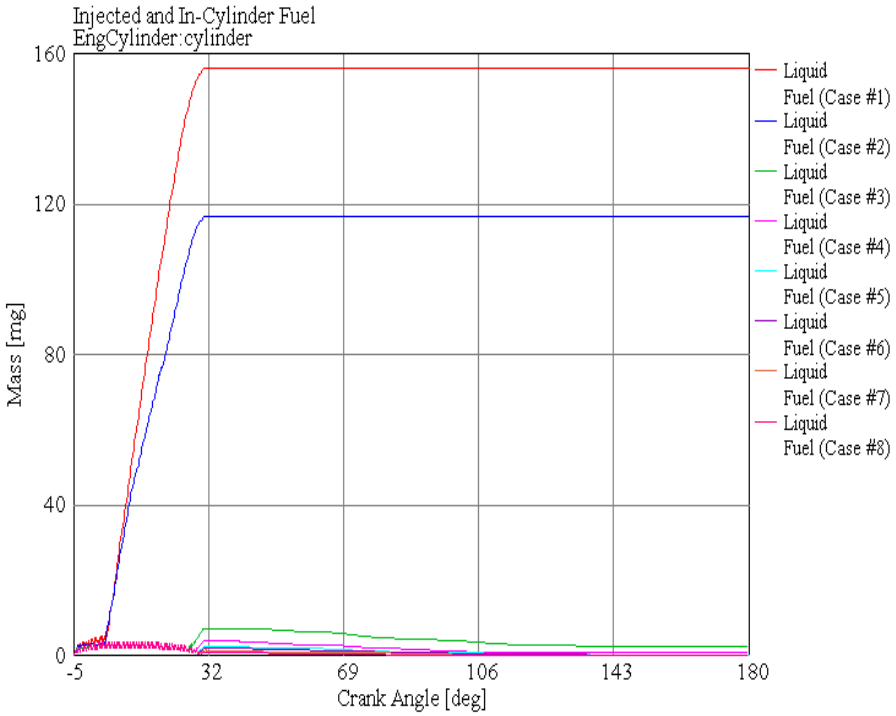

Fig. 11. In-cylinder liquid fuel of nozzle nine holes

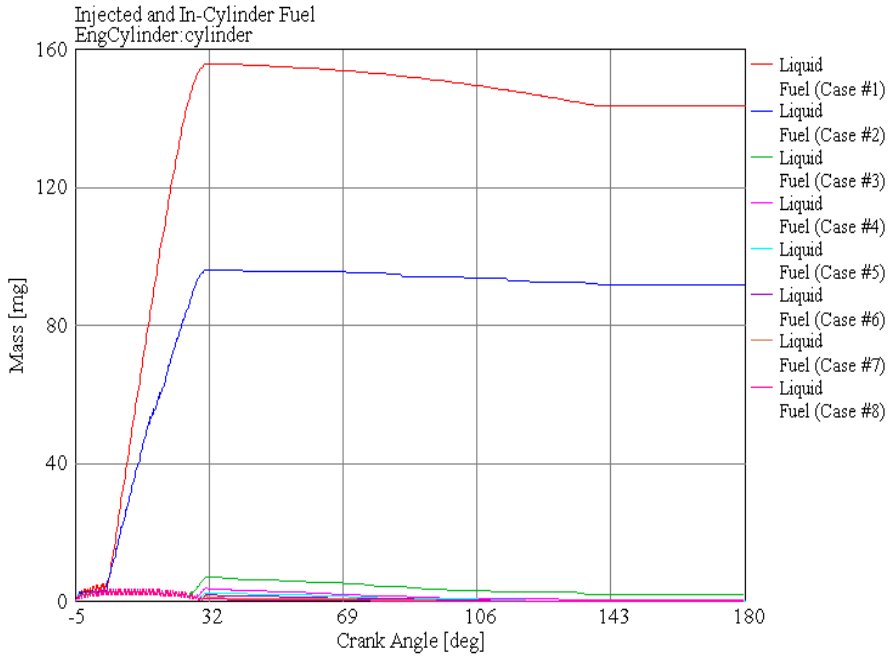

Fig. 12. In-cylinder liquid fuel of nozzle 10 holes

Fig. 12 illustrates the in-cylinder liquid fuel mass for a ten-hole nozzle configuration. Case #1 (red line) reaches a peak of around 155 mg near the 32° crank angle and shows a very slow decline, ending just above 130 mg at 180°, suggesting minimal evaporation. Case #2 (blue line) rises to approximately 90

mg and maintains a mostly stable mass with a slight downward trend, indicative of limited vaporization. Case #3 (green line) peaks under 10 mg and decreases slowly, while Cases #4 to #8 all stay under 5 mg, showing consistent and steady reduction across the crank cycle. This result demonstrates that even with a ten-hole nozzle, significant retention of liquid fuel occurs, particularly in Cases #1 and #2. This trend implies that increasing nozzle hole numbers beyond a certain threshold does not guarantee improved atomization or fuel-air mixing. Instead, it may worsen droplet penetration or lead to overlapping spray plumes, reducing evaporation efficiency. **Fig. 12** confirms that the optimal number of nozzle holes must consider spray dynamics and in-cylinder conditions, not just fuel delivery rate.

The optimal nozzle design would provide the maximum amount of liquid fuel burned in the combustion process and the minimum amount of liquid fuel unburned. Theoretically, a 10-hole nozzle satisfies this requirement. Unfortunately, jets emerging from a 10-hole nozzle tended to be very susceptible. All the nozzles were examined, and the result showed that the seven-hole nozzle provided the best results for any different engine speed in simulation and the best performance shown on a low-speed engine.

Nozzle Holes Effect on Engine Performance

The simulation result of the engine performance effect of fuel nozzle holes number and geometries in indicated power indicated torque, and ISFC of the engine is shown in **Fig. 13 – 15**. The simulation model running output shows the fuel nozzle hole orifice diameter and nozzle hole numbers, which indicate the power, torque, and ISFC performance of a direct-injection diesel engine. An aerodynamic interaction and turbulence affect spray breakup competently as the fuel nozzle hole orifice diameter decreases. The fuel drop size decreases if the fuel nozzle hole orifice diameter decreases, with a quantitative effect decreasing for a given set of jet conditions. Fuel-air mixing increases as the fuel nozzle holes and orifice diameter fuel nozzle holes decrease. Also, soot incandescence decreases as fuel-air premixing upstream of the lift-off length increases. This can be a significant advantage for small orifice nozzle holes. However, multiple holes orifice diameter is required to meet the desired mass flow rate as the orifice diameter decreases. In this case, the orifices' diameter must be placed with appropriate spacing and directions to avoid interference among adjacent sprays. The empirical correlations generally predict smaller drop size, slower penetrating speed and smaller spray cone angles as the orifice diameter decreases. However, the predicted values were different for different relations. All the nozzles examined showed that the five-hole nozzle provided the best results for indicted power, indicating torque and specific fuel consumption at any different engine speed in simulation.

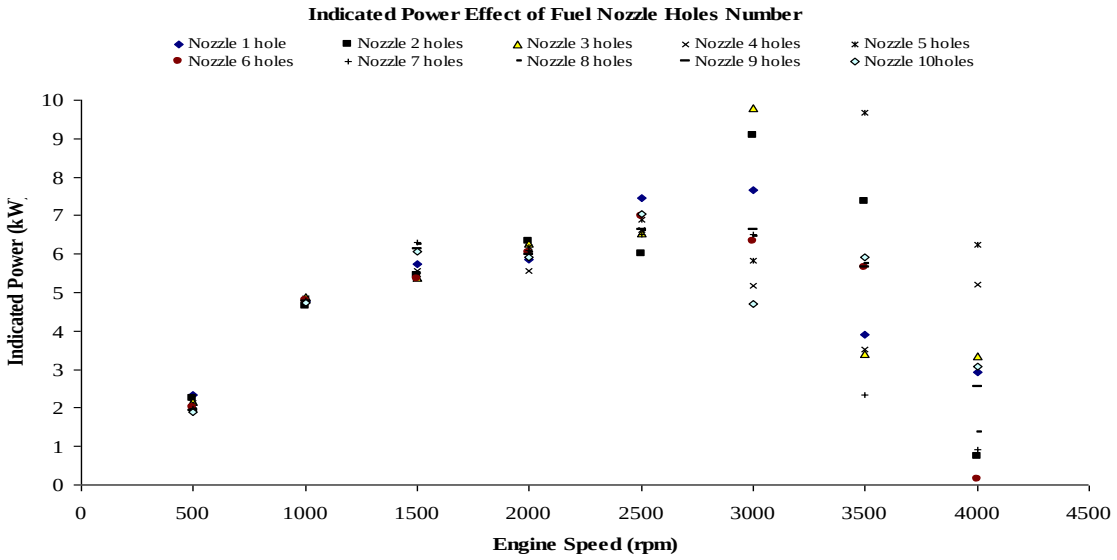

Fig. 13. Fuel nozzle holes effect on indicated power of an engine

Fig. 13 shows the effect of fuel nozzle hole numbers on the indicated power output of an engine at different engine speeds. Across all nozzle configurations, indicated power increases with engine speed up to around 2500 rpm, after which it starts to decline. The nozzle with three holes (△ symbol) achieves the highest indicated power, reaching nearly 9 kW at approximately 2500 rpm, outperforming other configurations. Meanwhile, configurations with one hole (◆ symbol) and five holes (× symbol) consistently deliver moderate indicated power values. Notably, the nozzles with six, seven, eight, nine, and ten holes demonstrate a faster drop-off in indicated power after reaching their peak, suggesting potential inefficiencies at higher speeds. At 4000 rpm, all nozzle configurations exhibit a significant drop in indicated power, with the six-hole nozzle (● symbol) showing the lowest power output, close to 1 kW. These results suggest that while an increase in nozzle hole number initially helps distribute fuel more effectively at moderate engine speeds, excessive numbers may impair combustion efficiency at high speeds due to over-atomization or poor air-fuel mixing. Therefore, an optimal number of nozzle holes (around three to five holes) seems crucial to maintaining high engine performance across various engine speeds.

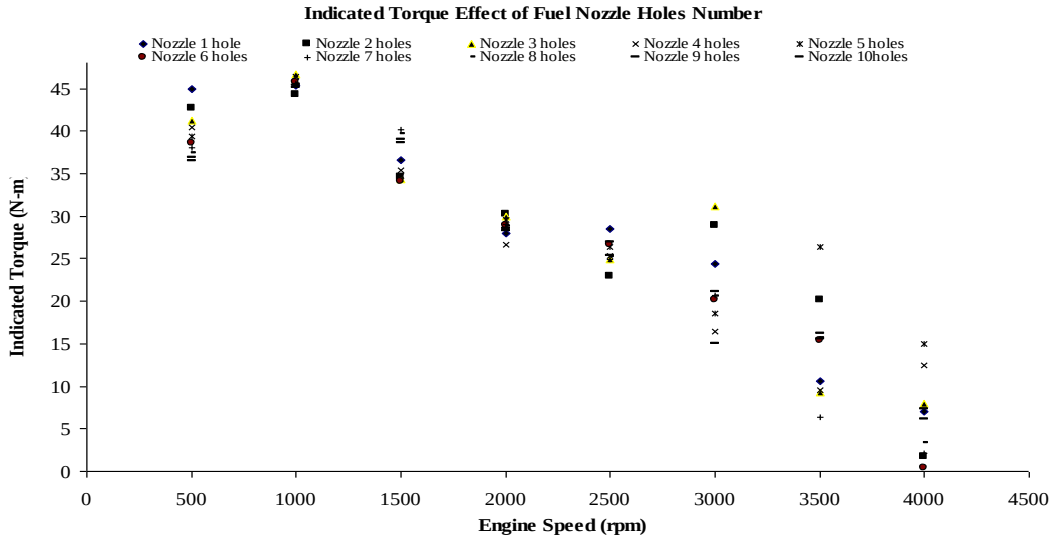

Fig. 14. Fuel nozzle holes effect on indicated torque of the engine

Fig. 14 shows the effect of fuel nozzle hole numbers on the indicated torque of the engine at different engine speeds. Overall, stated torque decreases as engine speed increases for all nozzle configurations. At low engine speeds (around 500 rpm and 1000 rpm), the indicated torque ranges between 40–45 N·m and is relatively similar across all nozzle designs. The three-hole nozzle (△ symbol) again stands out, maintaining the highest torque levels, especially at mid-range speeds (~2000 rpm and 2500 rpm) compared to other nozzle types. Beyond 3000 rpm, torque values drop sharply, with the nozzles with higher hole numbers (7–10 holes) experiencing a more significant decline. At 4000 rpm, many configurations approach near-zero torque output, particularly the six-hole nozzle (◆ symbol), which drops to almost 0 N·m, indicating poor combustion efficiency at high speeds. These results highlight that a moderate number of nozzle holes (around three to five) can maintain better combustion stability and torque generation across a broad engine speed range. In contrast, too many nozzle holes can degrade torque performance at higher rpm due to poor spray quality and air-fuel mixing.

Fig. 15 illustrates the effect of the number of fuel nozzle holes on an engine's indicated specific fuel consumption (ISFC) across different engine speeds. ISFC values remain relatively low at lower engine speeds (500–1500 rpm), ranging between 1400–1600 g/kWh across all nozzle configurations. As engine speed increases beyond 2000 rpm, ISFC values rise noticeably, indicating reduced fuel efficiency at higher speeds. Notably, the nozzles with three holes (△ symbol) and two holes (■ symbol) consistently show lower ISFC values than other configurations, suggesting better fuel economy performance. At high engine speeds (especially above 3000 rpm), the ISFC values for some configurations, particularly

the four-hole nozzle (× symbol), spike dramatically to above 4000 g/kWh, indicating abysmal fuel efficiency. The ten-hole nozzle (◇ symbol) and nozzles with higher hole numbers also exhibit higher ISFC at high rpm, reflecting inefficiencies caused by incomplete combustion or poor spray atomization. Thus, the data suggest that moderate nozzle configurations (two to three holes) optimize fuel usage better across a wide range of operating speeds. In contrast, higher-hole configurations worsen fuel consumption under high-load, high-speed conditions.

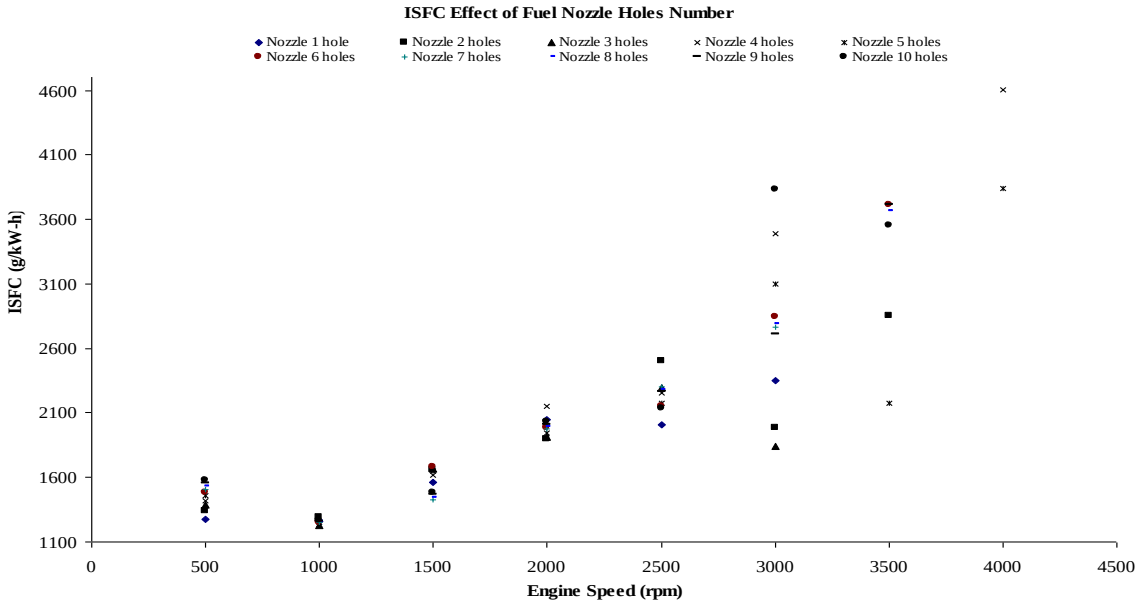

Fig. 15. Fuel nozzle holes effect on indicated specific fuel consumption of an engine

4. Conclusion

All the nozzles were examined, and the result showed that the seven-hole nozzle provided the best burning results for fuel in-cylinder burned at any different engine speed in simulation. The best burning was in low-speed engines. In the engine performance effect, all the nozzles were examined, and the five-hole nozzle provided the best results for indicated power, torque, and specific fuel consumption at any different engine speed in the simulation.

Acknowledgement

This research received no specific grant from funding agencies in the public, commercial, or not-for-profit sectors. The personal contributions of the authors solely supported the work.

References

Almardhiyah, F., Mahidin, M., Fauzi, F., Abnisa, F., & Khairil, K. (2025). Optimization of Aceh Low-Rank Coal Upgrading Process with Combination of Heating Media to Reduce Water Content through Response Surface Method. *International Journal of Science & Advanced Technology (IJSAT)*, 1(1), 29–37.

Bahagia, B., Nizar, M., Yasin, M. H. M., Rosdi, S. M., & Faisal, M. (2025). Advancements in Communication and Information Technologies for Smart Energy Systems and Renewable Energy Transition: A Review. *International Journal of Engineering and Technology (IJET)*, 1(1), 1–29.

Baik, S., Blanchard, J. P., & Corradini, M. L. (2003). Development of micro-diesel injector nozzles via microelectromechanical systems technology and effects on spray characteristics. *J. Eng. Gas Turbines Power*, 125(2), 427–434.

Bakar, R. A., & Semin, A. R. I. (n.d.). EFFECT OF ENGINE PERFORMANCE FOR FOUR-STROKE DIESEL ENGINE USING SIMULATION.

Baumgarten, C. (2006). *Mixture formation in internal combustion engines*. Springer Science & Business Media.

Febrina, R., & Anwar, A. (2025). Dynamic Modelling and Optimisation of Heat Exchange Networks for Enhanced Energy Efficiency in Industrial Processes. *International Journal of Simulation, Optimization & Modelling*, 1(1), 33–42.

Grimaldi, C. N., & Millo, F. (2015). Internal combustion engine (ICE) fundamentals. In *Handbook of clean energy systems* (Vol. 2, pp. 907–938). John Wiley & Sons Limited.

Heywood, J. B. (1988). *Internal Combustion Engine Fundamentals*. *McGrawHill series in mechanical engineering* (Vol. 21).

Iqbal, I., Rosdi, S. M., Muhtadin, M., Erdiwansyah, E., & Faisal, M. (2025). Optimisation of combustion parameters in turbocharged engines using computational fluid dynamics modelling. *International Journal of Simulation, Optimization & Modelling*, 1(1), 63–69.

Jalaludin, H. A., Kamarulzaman, M. K., Sudrajad, A., Rosdi, S. M., & Erdiwansyah, E. (2025). Engine Performance Analysis Based on Speed and Throttle Through Simulation. *International Journal of Simulation, Optimization & Modelling*, 1(1), 86–93.

Khalisha, N., Caisarina, I., & Fakhrana, S. Z. (2025). Mobility Patterns of Rural Communities in Traveling Traveling from The Origin Area to the Destination. *International Journal of Science & Advanced Technology (IJSAT)*, 1(1), 108–119.

Khanyi, N., Inambao, F. L., & Stopforth, R. (2025). A Comprehensive Review of the GT-POWER for Modelling Diesel Engines. *Energies*, 18(8), 1880.

Khayum, N., Goyal, R., & Kamal, M. (2025). Finite Element Modelling and Optimisation of Structural Components for Lightweight Automotive Design. *International Journal of Simulation, Optimization & Modelling*, 1(1), 78–85.

Kirkpatrick, A. T. (2020). *Internal combustion engines: applied thermosciences*. John Wiley & Sons.

Kumari, S., & Badholiya, S. K. (2020). A Study on Performance and Noise Analysis of 4 Stroke 4 Cylinder Diesel Engine.

Maulana, M. I., Rosdi, S. M., & Sudrajad, A. (2025). Performance Analysis of Ethanol and Fusel Oil Blends in RON95 Gasoline Engine. *International Journal of Automotive & Transportation Engineering*, 1(1), 81–91.

Muchlis, Y., Efriyo, A., Rosdi, S. M., & Syarif, A. (2025). Effect of Fuel Blends on In-Cylinder Pressure and Combustion Characteristics in a Compression Ignition Engine. *International Journal of Automotive & Transportation Engineering*, 1(1), 52–58.

Muchlis, Y., Efriyo, A., Rosdi, S. M., Syarif, A., & Leman, A. M. (2025). Optimization of Fuel Blends for Improved Combustion Efficiency and Reduced Emissions in Internal Combustion Engines. *International Journal of Automotive & Transportation Engineering*, 1(1), 59–67.

Mufti, A. A., Irhamni, I., & Darnas, Y. (2025). Exploration of predictive models in optimising renewable energy integration in grid systems. *International Journal of Science & Advanced Technology (IJSAT)*, 1(1), 47–61.

Muhibbuddin, M., Hamidi, M. A., & Fitriyana, D. F. (2025). Bibliometric Analysis of Renewable Energy Technologies Using VOSviewer: Mapping Innovations and Applications. *International Journal of Science & Advanced Technology (IJSAT)*, 1(1), 81–91.

Muhibbuddin, M., Muchlis, Y., Syarif, A., & Jalaludin, H. A. (2025). One-dimensional Simulation of Industrial Diesel Engine. *International Journal of Automotive & Transportation Engineering*, 1(1), 10–16.

Muhtadin, M., Rosdi, S. M., Faisal, M., Erdiwansyah, E., & Mahyudin, M. (2025). Analysis of NOx, HC, and CO Emission Prediction in Internal Combustion Engines by Statistical Regression and

ANOVA Methods. *International Journal of Simulation, Optimization & Modelling*, 1(1), 94–102.
Mutlu, M., & Kiliç, M. (2016). Effects of piston speed, compression ratio and cylinder geometry on system performance of a liquid piston. *Thermal Science*, 20(6), 1953–1961.
Muzakki, M. I., & Putro, R. K. H. (2025). Greenhouse Gas Emission Inventory at Benowo Landfill Using IPCC Method. *International Journal of Science & Advanced Technology (IJSAT)*, 1(1), 18–28.
Nizar, M., Syafrizal, S., Zikrillah, A.-F., Rahman, A., Hadi, A. E., & Pranoto, H. (2025). Optimizing Waste Transport Efficiency in Langsa City, Indonesia: A Dynamic Programming Approach. *International Journal of Science & Advanced Technology (IJSAT)*, 1(1), 10–17.
Nizar, M., Yana, S., Bahagia, B., & Yusop, A. F. (2025). Renewable energy integration and management: Bibliometric analysis and application of advanced technologies. *International Journal of Automotive & Transportation Engineering*, 1(1), 17–40.
NOOR, C. H. E. W. A. N. M., Arif, F., & Rusirawan, D. (2025). Optimising Engine Performance and Emission Characteristics Through Advanced Simulation Techniques. *International Journal of Simulation, Optimization & Modelling*, 1(1), 10–20.
Pranoto, H., Rusiyanto, R., & Fitriyana, D. F. (2025). Sustainable Wastewater Management in Sumedang: Design, Treatment Technologies, and Resource Recovery. *International Journal of Science & Advanced Technology (IJSAT)*, 1(1), 38–46.
Rajput, R. K. (2005). *Internal combustion engines*. Laxmi Publications.
Rosdi, S. M., Ghazali, M. F., & Yusop, A. F. (2025). Optimization of Engine Performance and Emissions Using Ethanol-Fusel Oil Blends: A Response Surface Methodology. *International Journal of Automotive & Transportation Engineering*, 1(1), 41–51.
Rosdi, S. M., Maghfirah, G., Erdiwansyah, E., Syafrizal, S., & Muhibbuddin, M. (2025). Bibliometric Study of Renewable Energy Technology Development: Application of VOSviewer in Identifying Global Trends. *International Journal of Science & Advanced Technology (IJSAT)*, 1(1), 71–80.
Rosdi, S. M., Yasin, M. H. M., Khayum, N., & Maulana, M. I. (2025). Effect of Ethanol-Gasoline Blends on In-Cylinder Pressure and Brake-Specific Fuel Consumption at Various Engine Speeds. *International Journal of Automotive & Transportation Engineering*, 1(1), 92–100.
Rosli, M. A., Xiaoxia, J., & Shuai, Z. (2025). Machine Learning-Driven Optimisation of Aerodynamic Designs for High-Performance Vehicles. *International Journal of Simulation, Optimization & Modelling*, 1(1), 43–53.
Salih, S., & DelVescovo, D. (2018). *Design and Validation of a GT Power Model of the CFR Engine towards the Development of a Boosted Octane Number*. Retrieved from SAE Technical Paper:
Sardjono, R. E., Khoerunnisa, F., Rosdi, S. M., & Muchlis, Y. (2025). Optimization of Engine Performance and Emissions with Fusel Oil Blends: A Response Surface Analysis on Speed and Throttle Parameters. *International Journal of Automotive & Transportation Engineering*, 1(1), 70–80.
Selvakumar, P., Maawa, W., & Rusiyanto, R. (2025). Hybrid Grid System as a Solution for Renewable Energy Integration: A Case Study. *International Journal of Science & Advanced Technology (IJSAT)*, 1(1), 62–70.
Semin, R. A. B., Ismail, A. R., & Ali, I. (2007). In An Engine Valve Lift Visualization And Simulation Performance Using CFD. In *Proceeding of Conference on Applications and Design in Mechanical Engineering (CADME), Malaysia*.
Smulter, B. (2024). Building a GT-Power-in-the-Loop System comprising a Fast-Running Model as an Extended Digital Twin for a Single-Cylinder Research Engine.
Sumarno, R. N., Fikri, A., & Irawan, B. (2025). Multi-objective optimisation of renewable energy systems using genetic algorithms: A case study. *International Journal of Simulation, Optimization & Modelling*, 1(1), 21–32.
Van Basshuysen, R., & Schäfer, F. (2016). *Internal combustion engine handbook*. SAE International.
Zhou, Y., Sofianopoulos, A., Lawler, B., & Mamalis, S. (2020). Advanced combustion free-piston engines: A comprehensive review. *International Journal of Engine Research*, 21(7), 1205–1230.